Computing 77, 29–55 (2006)
Digital Object Identifier (DOI) 10.1007/s00607-005-0150-2

Computing
Printed in Austria

Composite Finite Elements for Elliptic Boundary Value Problems with Discontinuous Coefficients

S. A. Sauter, Zürich, and **R. Warnke**, Ismaning

Received December 21, 2004; revised September 7, 2005
Published online: December 5, 2005

Abstract

In this paper, we will introduce composite finite elements for solving elliptic boundary value problems with discontinuous coefficients. The focus is on problems where the geometry of the interfaces between the smooth regions of the coefficients is very complicated.

On the other hand, efficient numerical methods such as, e. g., multigrid methods, wavelets, extrapolation, are based on a multi-scale discretization of the problem. In standard finite element methods, the grids have to resolve the structure of the discontinuous coefficients. Thus, straightforward coarse scale discretizations of problems with complicated coefficient jumps are not obvious.

In this paper, we define composite finite elements for problems with discontinuous coefficients. These finite elements allow the coarsening of finite element spaces independently of the structure of the discontinuous coefficients. Thus, the multigrid method can be applied to solve the linear system on the fine scale.

We focus on the construction of the composite finite elements and the efficient, hierarchical realization of the intergrid transfer operators. Finally, we present some numerical results for the multigrid method based on the composite finite elements (CFE–MG).

AMS Subject Classifications: 35J20, 65N15, 65N30.

Keywords: Composite finite elements, boundary values problems, discontinuous coefficients, multigrid methods.

1. Introduction

In many practical applications, partial differential equations with discontinuous coefficients have to be solved numerically. These coefficients represent the properties of the materials which may change discontinuously, e.g., in composite materials, by orders of magnitude.

Such problems are usually discretized via the finite element method. In standard finite element methods, the grid has to resolve the structure of the discontinuous coefficients. This condition links the minimal dimension of the finite element spaces directly to the number of discontinuities in the coefficients. On the other hand, the efficiency of many fast solution techniques as, e.g., multigrid methods, extrapolation, wavelets etc. depends on a multi-scale discretization of the problem.

In [10], [11], [12] and [19], *composite finite elements* are developed for the approximation of PDEs on complicated domains (see also [20] and [7]). These finite elements

allow coarse scale discretizations with the minimal number of unknowns not depending on the shape of the domain.

In this paper, we generalize the concept of composite finite elements to problems with discontinuous coefficients. As before, these finite elements can be used for coarsening finite element spaces and the coarse space dimension is independent of the structure of the discontinuous coefficients. In the context of the multigrid method, the coarse scale discretizations are employed to solve the linear system on the fine scale.

We compose the shape functions of a finite element on the coarse grids locally of piecewise polynomials on the elements of the finest grid. They are determined by solving locally the homogeneous PDE with suitable boundary conditions.

The concept of adapting the finite elements or, more generally, the ansatz functions to a given PDE is the basis for many discretization techniques (see, e. g., [2], [15], [13]). In [16], a multigrid algorithm is developed for periodic coefficients using homogenization techniques.

Our goal is to construct finite elements for *unstructured* discontinuous coefficients. This construction will be hierarchical. Thus, it can efficiently be used in a multigrid algorithm. Since the finite element functions on the coarser grids are combinations of the ones on the finer grids we call these finite elements *composite finite elements*. In the following, we denote the multigrid method based on these composite finite elements by CFE–MG.

In this paper, we concentrate on the construction of the composite finite elements and the efficient realization of the CFE–MG. In [21], we prove an approximation result for these finite elements in one dimension and, based on that, the convergence of the CFE–MG. The convergence rate is independent of the discontinuous coefficient. Thus, the total complexity of the multigrid method is linear in the degrees of freedom on the finest grid.

The paper is organized as followed. In Sect. 2, we formulate the model problem and its discretization, followed by a brief review to the multigrid method in Sect. 3. In Sect. 4, we define the composite finite elements for the one-dimensional problem and discuss its hierarchical realization. Section 5 is devoted to the two-dimensional problem. There, we will present a hierarchical construction of the composite finite elements. Additionally, we describe the efficient computation of these finite elements in the context of the multigrid method. Finally, in Sect. 6, we show some numerical results.

2. Model Problem and Discretization

Throughout this paper, we consider the problem

$$\begin{aligned} -\operatorname{div}(a \operatorname{grad} u) &= f \quad \text{in } \Omega \\ u &= 0 \quad \text{on } \partial\Omega \end{aligned}$$

as a model problem for elliptic boundary value problems. We assume that the coefficient a is discontinuous. The precise meaning of this problem with a discontinuous coefficient is given later in this section. We consider this problem on a bounded domain $\Omega \subset \mathbb{R}^d$ with a polygonal Lipschitz boundary $\partial\Omega$ for $d \in \{1, 2\}$. However, the definitions and algorithms for the two-dimensional problem can be transferred to three dimensions in a straightforward manner.

We presume that the coefficient a is piecewise constant. More precisely, let $q \in \mathbb{N}$ and $\mathcal{P} = \{\omega_i \subset \Omega : 1 \leq i \leq q\}$ be a finite set of disjoint subdomains with polygonal Lipschitz boundaries $\partial\omega_i$ such that

$$\bigcup_{\omega\in\mathcal{P}} \overline{\omega} = \overline{\Omega}\,.$$

Let $a \in L^\infty(\Omega)$ such that there is a family of real numbers $\{a_\omega\}_{\omega\in\mathcal{P}}$ with $a|_\omega = a_\omega$ for all $\omega \in \mathcal{P}$ and $a_{\min} := \min\{a_\omega : \omega \in \mathcal{P}\} > 0$. Therewith, we define the bilinear form

$$b : H_0^1(\Omega) \times H_0^1(\Omega) \to \mathbb{R};\ (u, v) \mapsto \int_\Omega a \,\langle \operatorname{grad} u, \operatorname{grad} v\rangle \, dx. \tag{1}$$

Obviously, b is symmetric, bounded and coercive by the Friedrichs inequality since we assume $a_{\min} > 0$. The variational formulation of the model problem reads as follows:

Problem 2.1: *Let $f \in H_0^1(\Omega)'$ be given. Find $u \in H_0^1(\Omega)$ such that*

$$b(u, v) = f(v)$$

holds for all $v \in H_0^1(\Omega)$.

The existence and uniqueness of Problem 2.1 is ensured by the Lax-Milgram theorem.

We denote the internal boundary, the so called *interfaces*, by

$$\gamma := \Omega \cap \bigcup_{\omega\in\mathcal{P}} \partial\omega \tag{2}$$

and the jump of a function u in $x \in \gamma$ by $[u](x)$.

In [3], sufficient conditions on the regularity of the interfaces γ are given such that the variational Problem 2.1 is equivalent to a strong formulation with interface conditions.

We approximate the solution of Problem 2.1 by the solution of a discrete, finite dimensional problem which is obtained by *Galerkin discretization*. Therefore, we replace the infinite dimensional space $H_0^1(\Omega)$ in Problem 2.1 by a finite dimensional subspace $\mathcal{S} \subset H_0^1(\Omega)$. This subspace is given by finite elements. Then, the discrete problem reads as follows.

Problem 2.2: *Let $f \in H_0^1(\Omega)'$ be given. Find $u_{\mathcal{S}} \in \mathcal{S}$ such that*

$$b(u_{\mathcal{S}}, v) = f(v)$$

holds for all $v \in \mathcal{S}$.

3. Multigrid Method

Let $\{\varphi_x\}_{x\in\Theta}$ be a basis of $\mathcal{S}$ for some index set Θ. Then, we define the *system matrix* $A_{xy} := b(\varphi_y, \varphi_x)$ and the right-hand side $F_x := f(\varphi_x)$ for all $x, y \in \Theta$. Thus, Problem 2.2 is equivalent to: Find $U \in \mathbb{R}^\Theta$ such that

$$A\,U = F. \tag{3}$$

The solution U of (3) and $u_{\mathcal{S}}$ of Problem 2.2 are linked via

$$u_{\mathcal{S}} = \sum_{y\in\Theta} U_y\,\varphi_y.$$

Using, e. g., the linear hat functions as the basis $\{\varphi_x\}_{x\in\Theta}$ on a grid $\mathcal{G}$ with the set of interior nodes Θ yields a sparse system matrix A of, typically, very large dimension. Thus, iterative solvers have to be employed for solving the linear system. In this paper, we use the multigrid method as an efficient iterative method to solve large sparse systems as in (3).

Under mild conditions, each iteration step of the multigrid method has a complexity which is linear in the number of unknowns. If, additionally, the convergence rate is bounded below away from 1, the system can be solved with linear complexity up to a given precision.

The key ingredients of the multigrid method are:

- a hierarchy of discretizations (given, e. g., by finite elements on a hierarchy of grids),
- prolongation and restriction operators P_l^{l+1}, R_{l+1}^l which interfere between the discretizations, and
- smoothing operators S_l for the discretizations.

Typically, the hierarchy of discretizations is obtained via a nested hierarchy of grids $\{\mathcal{G}_l\}_{l=0}^L$ and the finite element basis functions $\{\varphi_x^l\}_{x\in\Theta_l}$ on the grids $\mathcal{G}_l$. The prolongation and restriction operators are defined by

$$\begin{aligned} P_l^{l+1} &: \mathbb{R}^{\Theta_l} \to \mathbb{R}^{\Theta_{l+1}}; \\ \left(P_l^{l+1}U\right)_x &:= \textstyle\sum_{y\in\Theta_l} \varphi_y^l(x)\,U_y \quad \text{for all } x \in \Theta_{l+1} \end{aligned} \tag{4}$$

and

$$\begin{aligned} R_{l+1}^l &:= \left(P_l^{l+1}\right)^T : \mathbb{R}^{\Theta_{l+1}} \to \mathbb{R}^{\Theta_l}; \\ \left(R_{l+1}^l U\right)_x &:= \textstyle\sum_{y\in\Theta_{l+1}} \varphi_x^l(y)\,U_y \quad \text{for all } x \in \Theta_l. \end{aligned} \tag{5}$$

We simply replace the hat basis $\{\varphi_x\}_{x\in\Theta}$ by the composite finite element basis for the definition of the prolongation and restriction operators in the CFE–MG.

Finally, the multigrid method requires smoothing operators

$$S_l : \mathbb{R}^{\Theta_l} \to \mathbb{R}^{\Theta_l}, \quad 0 \le l \le L,$$

on the grid hierarchy. For simplicity, we consider here only classical iteration methods as the damped Jacobi iteration or the (symmetric) Gauß-Seidel iteration.

Multigrid algorithm 3.1: Let $\nu_1, \nu_2 \in \mathbb{N}_0$ be the number of pre- respectively post-smoothing steps, let $\mu \in \{1, 2\}$ and $0 \le l \le L$. Let $U^0 \in \mathbb{R}^{\Theta_l}$ be a starting guess, e. g., $U^0 = 0$ or determined by a nested iteration.

Let $i \in \mathbb{N}$ and assume that U^{i-1} is given. If $l = 0$ set $U^i := A_0^{-1} F$. Otherwise, compute U^i by an iteration of the multigrid method, i. e.,

(1) perform ν_1 pre-smoothing steps $W := S_l^{\nu_1} U^{i-1}$,
(2) compute the restriction of the residuum $D := R_l^{l-1}\big(A_l W - F\big)$,
(3) perform μ iterations of this algorithm with $l-1$ instead of l, D instead of F and the initial vector $V^0 = 0$. The result is denoted by V^μ,
(4) set $W := U^{i-1} - P_{l-1}^l V^\mu$ and
(5) perform ν_2 post-smoothing steps $U^i := S_l^{\nu_2} W$.

Since the system matrix A_l is sparse, the complexity of a multiplication with A_l is of order $O(\#\Theta_l)$. Thus, the complexity of the damped Jacobi iteration or the (symmetric) Gauß-Seidel iteration is of order $O(\#\Theta_l)$ as well. Typically, in particular for the prolongation and restriction in (4) respectively (5), the complexity of Algorithm 3.1 (2) and (4) is of order $O(\#\Theta_l)$ each.

If $\max\left\{\frac{\#\Theta_l}{\#\Theta_{l+1}} : 0 \le l < L\right\} < 1$ and $A_0^{-1} F$ is solved with constant complexity, then, the complexity of one iteration of Algorithm 3.1 is of order $O\big((\nu_1 + \nu_2)\,\#\,\Theta_l\big)$. For a proof, see [8].

4. Composite Finite Elements in One Dimension

Due to the lack of regularity, standard finite elements are not suited for the approximation of Problem 2.1, see [4]. Our goal is to adapt the shape of the finite elements to the solution of Problem 2.1.

More precisely, we solve the homogeneous problem, i. e., Problem 2.1 with $f = 0$, on local neighbourhoods about the elements T of the grid $\mathcal{G}$ and compose these solutions with suitable boundary conditions to globally continuous finite elements. These finite elements are a generalization of the linear finite elements in the sense that they reduce to linear elements for constant coefficients. For related approaches we refer to [2], [13], [15].

Let $\mathcal{G}$ be a grid for $\Omega = (\alpha, \beta) \subset \mathbb{R}$ and let Θ be the set of nodes of $\mathcal{G}$. We emphasize that the interface γ may not be resolved by the nodes Θ. We assume, that the elements $T \in \mathcal{G}$ are open such that $\Theta \cap \overline{T}$ consists of the endpoints of T and $\gamma \cap T$ of the inner interfaces with respect to T.

Throughout the paper, we use the following notation. For a grid $\mathcal{G}$ with nodes Θ, $\{\varphi_x\}_{x\in\Theta}$ denotes the standard "hat" functions while the basis of the composite finite elements will be denoted by $\{\psi_x\}_{x\in\Theta}$.

The finite element function ψ_x, $x \in \Theta$, restricted to $T \in \mathcal{G}$, will be the unique solution of the local and homogeneous PDE

$$\begin{aligned} -a_i\, \psi_x'' &= 0 && \text{in } \omega \cap T \text{ for all } \omega \in \mathcal{P} \text{ with } \omega \cap T \neq \emptyset, \\ \left[a\, \psi_x'\right] = [\psi_x] &= 0 && \text{on } \gamma \cap T, \\ \psi_x(y) &= \delta_{xy} && \text{for all } y \in \Theta \cap \overline{T}. \end{aligned} \tag{6}$$

It turns out that, for the generalization of this definition to the two-dimensional case, it is preferable to reformulate (6) in a variational way.

Definition 4.1: *For all $x \in \Theta$ and all $T \in \mathcal{G}$, let $u_{x,T} \in H_0^1(T)$ be the solution of*

$$b(u_{x,T}, v) = -b(\varphi_x, v) \tag{7}$$

for all $v \in H_0^1(T)$. Then, the basis functions are given by

$$\psi_x|_T := u_{x,T} + \varphi_x|_T$$

and the space of composite finite elements *by*

$$\mathcal{S}^{\mathrm{CFE}} := \operatorname{span}\{\psi_x : x \in \Theta\} \subset H^1(\Omega).$$

We call this finite elements *composite finite elements* as they are a linear combination of linear finite elements on the mesh which is induced by the set of nodes $\Theta \cup \gamma$. In the hierarchical representation of these finite elements, the elements on the coarser grids are a linear combination of elements on the finer grids. Thus, they are hierarchically composed of elements with respect to the set of nodes $\Theta \cup \gamma$.

In Fig. 1, a basis function ψ_{x_2} is depicted for a characteristic example.

Lemma 4.2: *For all $x \in \Theta$ and all $T \in \mathcal{G}$, $\psi_x|_T$ solves* (6) *uniquely.*

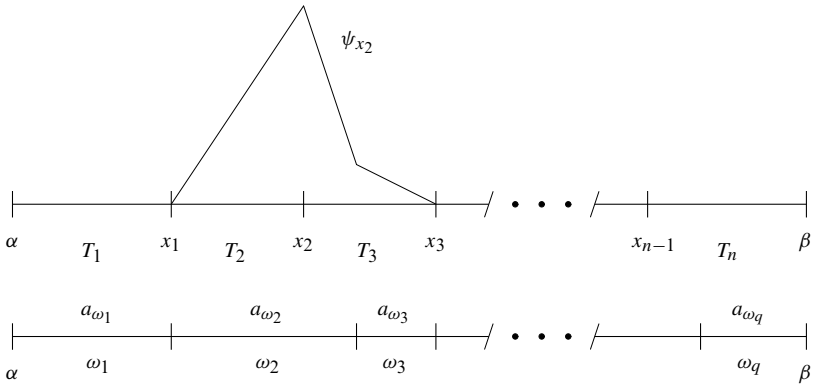

Fig. 1. Illustration of a basis function ψ_{x_2}. The grid $\mathcal{G} = \{T_1, \ldots, T_n\}$ does not resolve the interfacial points of the coefficient a

Remark 4.3:

(1) For all $x \in \Theta$, it holds

$$\operatorname{supp} \psi_x = \operatorname{supp} \varphi_x = \bigcup \{\overline{T} : T \in \mathcal{G} \text{ with } x \in \overline{T}\}.$$

(2) For all $x \in \Theta$ and all $T \in \mathcal{G}$, the product $\left(a\, \psi_x'|_T\right)$ is constant.
(3) In the case of a constant coefficient a, it holds $\psi_x = \varphi_x$ for all $x \in \Theta$.
(4) $\{\psi_x\}_{x\in\Theta}$ is a partition of unity on Ω.

The construction of the composite finite elements allows to define a hierarchy of discretizations for Problem 2.1. The dimension of the coarsest one is very small and independent of the number and structure of the interfaces γ. In order to use them in a multigrid algorithm it is essential to define, in addition, local intergrid operators which will be done next.

Let $L \in \mathbb{N}$ and let $\{\mathcal{G}_l\}_{l=0}^{L}$ be a hierarchy of grids on Ω. The index L corresponds to the finest and the index 0 to the coarsest grid. Let Θ_l be the set of nodes of grid $\mathcal{G}_l$.

We assume that this hierarchy of grids is nested, i. e., for $0 \leq l < L$, it holds

$$\Theta_l \subset \Theta_{l+1}. \tag{8}$$

The set of *successors* of an element $T^l \in \mathcal{G}_l$ is given by

$$\operatorname{sons}(T^l) := \left\{T^{l+1} \in \mathcal{G}_{l+1} : T^{l+1} \subset T^l\right\} \subset \mathcal{G}_{l+1}.$$

By Lemma 4.2, the basis functions $\left\{\psi_x^l\right\}_{x\in\Theta_l}$ (cf. Definition 4.1) satisfy (6) for all $T^l \in \mathcal{G}_l$. The basis functions ψ_y^{l+1} on the next finer grid satisfy (6) with $T = T^{l+1} \in \operatorname{sons}(T^l)$ for all $y \in \Theta_{l+1} \cap \overline{T^l}$. This leads to the hierarchical ansatz

$$\psi_x^l = \sum_{y\in\Theta_{l+1}\cap\overline{T^l}} \alpha_{xy}\,\psi_y^{l+1}. \tag{9}$$

Relation (9) is a local hierarchical ansatz and it remains to determine the coefficients α_{xy} such that ψ_x^l satisfies (6) at the nodes $y \in \Theta_{l+1} \cap \overline{T^l}$ as well.

This leads to uniquely solvable linear systems with dimension $\#\big(\Theta_{l+1}\cap\overline{T^l}\big)$. In particular, the dimension is very small and independent of the coefficient a (cf. (12)).

Definition 4.1 is equivalent to the following recursion.

Lemma 4.4: *Let $0 \le l < L$. Then, for all $x \in \Theta_l$ and all $T \in \mathcal{G}_l$, it holds*

$$\psi_x^l|_T = u_{x,T}^l + \psi_x^{l+1}|_T \tag{10}$$

where $u_{x,T}^l \in \mathcal{S}_{l+1}^{\mathrm{CFE}} \cap H_0^1(T)$ is the solution of

$$b(u_{x,T}^l, \psi_y^{l+1}) = -b(\psi_x^{l+1}, \psi_y^{l+1}) \tag{11}$$

for all $y \in \Theta_{l+1} \cap T$.

Proof: We denote the function defined by (10) and (11) by $\xi_x^l|_T := u_{x,T}^l + \psi_x^{l+1}|_T$ and show $\xi_x^l|_T = \psi_x^l|_T$, i.e., ξ_x^l satisfies (7). The interpolation onto the space $\mathcal{S}^{\mathrm{CFE}}$ is defined by

$$\mathcal{I}^{\mathrm{CFE}} : H^1(\Omega) \to \mathcal{S}^{\mathrm{CFE}}; \quad u \mapsto \sum_{x\in\Theta} u(x)\,\psi_x$$

which is well defined on $H^1(\Omega)$ in one dimension by Sobolev's theorem. Let $x \in \Theta_l$, $T \in \mathcal{G}_l$ and $v_T \in H_0^1(T)$. For all $t \in \mathrm{sons}(T) \subset \mathcal{G}_{l+1}$, set

$$u_t := (v_T - \mathcal{I}_{l+1}^{\mathrm{CFE}} v_T)|_t \in H_0^1(t).$$

We extend the functions v_T and u_t by 0 to Ω. It follows

$$v_T = \mathcal{I}_{l+1}^{\mathrm{CFE}} v_T + \sum_{t\in\mathrm{sons}(T)} u_t$$

and consequently

$$b(\xi_x^l, v_T) = \sum_{y\in\Theta_{l+1}\cap T} v_T(y)\, b(\xi_x^l, \psi_y^{l+1}) + \sum_{t\in\mathrm{sons}(T)} b(\xi_x^l, u_t).$$

Equation (11) implies $b(\xi_x^l, \psi_y^{l+1}) = 0$ for all $y \in \Theta_{l+1} \cap T$ and the first sum vanishes. Furthermore, it holds $\xi_x^l \in \mathcal{S}_{l+1}^{\mathrm{CFE}}$ and we can represent ξ_x^l by the functions ψ_y^{l+1} which satisfy Definition 4.1. Choosing v in Definition 4.1 as u_t leads to $b(\xi_x^l, u_t) = 0$ for all $t \in \mathrm{sons}(T)$ and also the second sum vanishes. □

The essential difference of Lemma 4.4 and Definition 4.1 is that the ansatz and test spaces in (11) are not $H_0^1(T)$ but only $\mathcal{S}_{l+1}^{\mathrm{CFE}}|_T \cap H_0^1(T)$. Thus, (11) is equivalent to a system of linear equations with a dimension that does not depend on a.

The coefficients α_{xy} in (9) can be computed as follows. In the end points x, y of an element $T = (x, y) \in \mathcal{G}_l$ it holds $\alpha_{xx} = 1$ and $\alpha_{xy} = 0$. For an inner point $z \in \Theta_{l+1} \cap T$, α_{xz} is determined by the linear system in (11). The coefficients $b(\psi_x^{l+1}, \psi_y^{l+1}) = (A_{l+1})_{yx}$ of these equations are given by the elements of the system matrix A_{l+1} corresponding to the grid $\mathcal{G}_{l+1}$.

Usually, the one-dimensional grid hierarchy for the multigrid method arises from recursive bisections of the elements. Thus, the linear system in (11) has dimension one and the solution is given by

$$\alpha_{xy} = \psi_x^l(y) = -\frac{b(\psi_x^{l+1}, \psi_y^{l+1})}{b(\psi_y^{l+1}, \psi_y^{l+1})}. \tag{12}$$

Since we have $\psi_x^l|_T = u_{x,T}^l + \psi_x^{l+1}|_T \in \mathcal{S}_{l+1}^{\mathrm{CFE}}$ the composite finite element spaces are nested, i. e.,

$$S_l^{\mathrm{CFE}} \subset S_{l+1}^{\mathrm{CFE}}. \tag{13}$$

5. Composite Finite Elements in Two Dimensions

Analogously to the one-dimensional problem, we solve the homogeneous PDE locally for the construction of the composite finite element basis functions in two dimensions. In contrast to the one-dimensional problems, these local problems along with the Lagrange property for the nodal basis do not define the functions uniquely since no boundary values are prescribed in the open interior of the boundary edges of the elements.

Therefore, we impose artificial boundary conditions on the boundary of an element neighborhood which we call "security zone". Similarly to PUFEM (partition of unity finite element method), see [17], we localize the solutions of these boundary value problems and utilize them for the finite elements. This gives us a hierarchical construction of the finite elements which can efficiently be combined with the multigrid method.

In Subsect. 5.1, the construction of a hierarchy of finite elements is presented, followed by some basic properties for these finite elements in Subsect. 5.2. In Subsect. 5.4, the efficient realization of the CFE–MG will be described.

5.1. Construction of Composite Finite Elements

Let $L \in \mathbb{N}$ and let $\{\mathcal{G}_l\}_{l=0}^L$ be a hierarchy of grids on Ω (see Sect. 2) such that $\mathcal{G}_L$ is the finest and $\mathcal{G}_0$ the coarsest grid. Let Θ_l be the set of nodes of grid $\mathcal{G}_l$. We use

the notation $\{\varphi_x^l\}_{x\in\Theta_l}$ for the basis of the linear finite elements on the grid $\mathcal{G}_l$ and $\{\psi_x^l\}_{x\in\Theta_l}$ for the composite finite element basis.

Assumption 5.1: *The finest grid $\mathcal{G}_L$ resolves the geometry of the internal boundary γ, i. e.,*

$$\gamma \subset \bigcup_{T\in\mathcal{G}_L} \partial T.$$

The grid hierarchy is nested, i. e., for all $0 \le l < L$ and all $T \in \mathcal{G}_l$, there exists a set $\mathrm{sons}(T) \subset \mathcal{G}_{l+1}$ *such that*

$$\overline{T} = \bigcup_{t\in\mathrm{sons}(T)} \bar{t}. \tag{14}$$

By (14), the sets of nodes Θ_l are nested, i. e.,

$$\Theta_{l-1} \subset \Theta_l.$$

We say, a grid $\mathcal{G}$ "almost resolves" the polygonal interfaces γ if the elements $T \in \mathcal{G}$ can be subdivided into $O(1)$ successors $\mathrm{sons}(T)$ such that the refined grid resolves γ (see Fig. 2). A grid hierarchy satisfying Assumption 5.1 can, for instance, be obtained by the following algorithm. A starting grid $\mathcal{G}_0$ is refined by congruent refinement (connecting midpoints of edges) until it almost resolves γ yielding the grid $\mathcal{G}_{L-1}$. Finally, $\mathcal{G}_L$ is the subdivision of $\mathcal{G}_{L-1}$ such that γ is resolved.

The construction of the composite finite element basis functions is hierarchical and starts from the finest grid of the hierarchy. By Assumption 5.1, $\mathcal{G}_L$ resolves γ. Thus, we set

$$\mathcal{S}_L^{\mathrm{CFE}} := \mathcal{S}_L = \big\{v \in C(\Omega) : \forall T \in \mathcal{G}_L : v|_T \in \mathcal{P}_1\big\}.$$

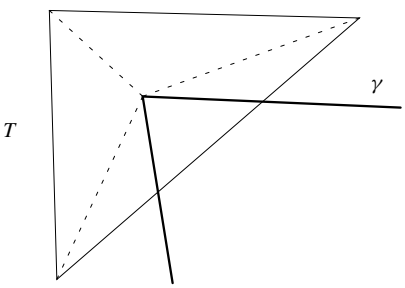

Fig. 2. An element T for which the two connectivity components of $T\backslash\gamma$ can be subdivided into 5 successors such that $\gamma \cap T$ is resolved

If we assume that $\mathcal{S}_{l+1}^{\mathrm{CFE}}$ is already defined we can, analogously to (9), make the ansatz for the coarser basis functions for each element $T^l \in \mathcal{G}_l$:

$$\psi_x^l|_{T^l} = \sum_{y \in \Theta_{l+1} \cap \overline{T^l}} \alpha_{xy}\, \psi_y^{l+1}|_{T^l}. \tag{15}$$

We will construct these finite elements such that the following properties hold:

(a) On the elements $T \in \mathcal{G}_l$, they solve the local homogeneous equation related to the bilinear form $b(\cdot, \cdot)$ as in (1).
(b) They form a Lagrange basis.
(c) They have local support $\operatorname{supp} \psi_x^l \subset \bigcup \{\overline{T} : T \in \mathcal{G}_l \text{ with } x \in \overline{T}\}$.

The coefficients α_{xy} are determined in three steps:

(1) Setting up local problems (security zones and boundary condition),
(2) Solving these local problems,
(3) Composing the local solutions to globally continuous basis functions.

5.1.1. Setting Up Local Problems (Step 1)

In one dimension, the boundary values (values at the interval endpoints) of the local problems on the elements are canonically given by the Lagrange property of the finite elements. In the two-dimensional case, we have to impose artificial boundary values at the interior of the element edges. Since these artificial boundary conditions, in general, do not reflect the possibly oscillating behaviour of the solutions, we reduce their influence by imposing them at the boundary of the security zones, which are sufficiently far from T. Numerical experiments show (cf. Sect. 6) that, at most, three layers of triangles about T are sufficient to define the security zone for T. The concept of security zones for the construction of generalized finite elements is employed in [2], [13], [15] as well.

For $\omega \subset \overline{\Omega}$, let

$$\mathcal{G}_l^{\omega,0} := \{\omega\}$$

and, for all $k \in \mathbb{N}$, we define "triangle layers" about ω by (see Fig. 3)

$$\mathcal{G}_l^{\omega,k} := \left\{ T \in \mathcal{G}_l : \exists S \in \mathcal{G}_l^{\omega,k-1} : \overline{T} \cap \overline{S} \neq \emptyset \right\} \subset \mathcal{G}_l.$$

Finally, we denote the domain of $\mathcal{G}_l^{\omega,k}$ by

$$\operatorname{dom}(\mathcal{G}_l^{\omega,k}) := \operatorname{int}\left(\bigcup \{\overline{T} : T \in \mathcal{G}_l^{\omega,k}\} \right).$$

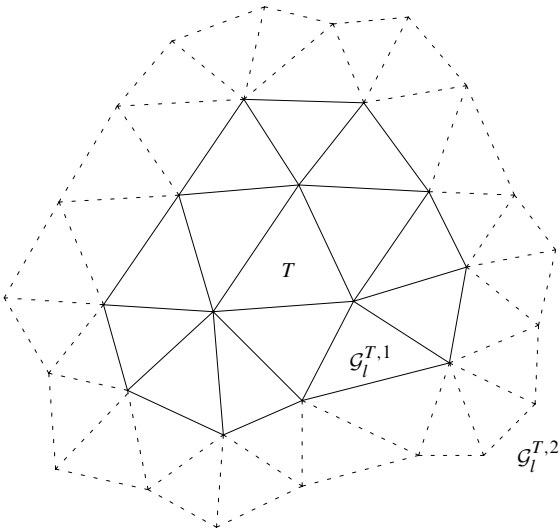

Fig. 3. The subgrids $\mathcal{G}_l^{T,1}$ and $\mathcal{G}_l^{T,2}$ for $T \in \mathcal{G}_l$

The construction of the finite elements is recursive starting on the finest grid. We assume that the basis $\{\psi_x^{l+1}\}_{x\in\Theta_{l+1}}$ is defined. In the following, we will construct the basis $\{\psi_x^l\}_{x\in\Theta_l}$. The interpolation $\mathcal{I}_{l+1}^{\mathrm{CFE}}$ onto $\mathcal{S}_{l+1}^{\mathrm{CFE}}$ is given by

$$\mathcal{I}_{l+1}^{\mathrm{CFE}} : C(\overline{\Omega}) \to \mathcal{S}_{l+1}^{\mathrm{CFE}}; \quad u \mapsto \sum_{x\in\Theta_{l+1}} u(x)\,\psi_x^{l+1}. \tag{16}$$

Let $k \in \mathbb{N}_0$. For the security zone of the element $T \in \mathcal{G}_l$, we use

$$U_T := \mathrm{dom}(\mathcal{G}_l^{T,k}). \tag{17}$$

In order to obtain three linearly independent shape functions on each element T, we choose three linearly independent functions on ∂U_T. For a vertex x of T, let $p_{x,T}^l \in \mathcal{P}_1$ be the (unique) affine extension of the standard shape function $\varphi_x^l|_T$ to a function on $\mathbb{R}^2$ and

$$g_{x,T}^l := \big(\mathcal{I}_{l+1}^{\mathrm{CFE}} p_{x,T}^l\big)\big|_{U_T} \tag{18}$$

the interpolation in $\mathcal{S}_{l+1}^{\mathrm{CFE}}|_{U_T}$. In particular, $g_{x,T}^l$ interpolates $p_{x,T}^l$ in the vertices of T.

This leads to the following local boundary value problem. For each vertex x of T, find $u_{x,T}^l \in S_{l+1}^{\mathrm{CFE}} \cap H_0^1(U_T)$ such that

$$b(u_{x,T}^l, v) = -b(g_{x,T}^l, v) \tag{19}$$

holds for all $v \in S_{l+1}^{\mathrm{CFE}} \cap H_0^1(U_T)$.

5.1.2. Solving (Step 2)

Let θ_T denote the set of vertices of a triangle T. The problem (19) has a unique solution $u^l_{x,T} \in S^{\mathrm{CFE}}_{l+1} \cap H^1_0(U_T)$ for all $x \in \theta_T$. Therefore, the functions

$$\xi^l_{x,T} := u^l_{x,T} + g^l_{x,T} \in S^{\mathrm{CFE}}_{l+1}|_{U_T} \tag{20}$$

solve the homogeneous equations associated with the bilinear form b and have the boundary values $\xi^l_{x,T} = g^l_{x,T}$ on ∂U_T.

However, these solutions, in general, are not a Lagrange basis on T, i. e., they do not interpolate $(\delta_{xy})_{y\in\theta_T}$ with the Kronecker delta δ_{xy}. Because the boundary values $g^l_{x,T}|_{\partial U_T}$ are linearly independent, the Lagrange property can be satisfied by a simple normalization: There exist coefficients $\beta^l_{xy} \in \mathbb{R}$ for the vertices $x, y \in \theta_T$ such that the functions

$$\zeta^l_{x,T} := \sum_{y\in\theta_T} \beta^l_{xy}\, \xi^l_{y,T} \in S^{\mathrm{CFE}}_{l+1}|_{U_T} \tag{21}$$

fulfil the equations $\zeta^l_{x,T}(y) = \delta_{xy}$ for all $x, y \in \theta_T$. Thus, $\left(\zeta^l_{x,T}|_T\right)_{x\in\theta_T}$ is a local Lagrange basis on T.

5.1.3. Composing (Step 3)

In this last step, we restrict the functions $\zeta^l_{x,T}$ to the elements T and compose the global basis functions. In general, however, the functions on neighbouring elements do not coincide along common edges such that

$$\sum_{T\in\mathcal{G}^{x,1}_l} \zeta^l_{x,T}|_T$$

does not give a continuous basis function for $x \in \Theta_l$. In order to obtain conforming finite element functions we average the functions on the element edges. More precisely, the values of the coarsened finite element function ψ^l_x, at the fine grid nodes y will be a weighted average of the (discontinuous) values of the functions $\zeta^l_{x,T}$ in these nodes and we employ the general ansatz

$$\psi^l_x(y) = \sum_{T\in\mathcal{G}^{y,1}_l} \alpha^l_{x,T,y}\zeta^l_{x,T}(y)\,.$$

Once, the coefficients $\psi^l_x(y)$ have been fixed, the composite finite element basis functions are determined by formula (15) with the choice $\alpha_{xy} := \psi^l_x(y)$. In the following, we will define the averaging coefficients $\alpha^l_{x,T,y}$.

The internal boundary γ is part of the Lipschitz boundaries of the inclusions Ω_i, $i \in N$, and, by Assumption 5.1, part of the edges of $\mathcal{G}_L$. Hence, there exists a piecewise constant, oriented normal vector field

$$\nu : \gamma \to \mathbb{S}^1 \subset \mathbb{R}^2$$

almost everywhere on γ. For all $T \in \mathcal{G}_l$ and its vertices x, we define the weights $[\alpha^l_{x,T}]$ by the jumps which are averaged over a triangle according

$$[\alpha^l_{x,T}] := \Big| \int_{\gamma \cap T} [a] [\partial_\nu \zeta^l_{x,T}] \, d\sigma \Big|. \tag{22}$$

At the end of this section, we motivate the choice of the weights in the case of laminar interfaces. The factor $[a]$ excludes "artificial" interfaces where the coefficient a crosses continuously.

For all $0 \le l < L$ and all $x \in \Theta_l$, set (see Fig. 4)

$$\theta^x_{l+1} := \{x\} \cup \big((\Theta_{l+1} \setminus \Theta_l) \cap \operatorname{dom}(\mathcal{G}^{x,1}_l) \big).$$

We define the basis functions ψ^l_x at $y \in \theta^x_{l+1}$ by the weighted averages of the functions $\zeta^l_{x,T}$ of the elements $T \in \mathcal{G}^{y,1}_l$. In case of $[\alpha^l_{x,T}] = 0$ (which happens, e. g., for a constant coefficient a), we return to unweighted averages which is reflected in the definition

$$\alpha^l_{x,T,y} := \begin{cases} 1 & \text{for } \Big| \sum_{T \in \mathcal{G}^{y,1}_l} [\alpha^l_{x,T}] \Big| < \text{tol}, \\ [\alpha^l_{x,T}] & \text{otherwise}, \end{cases}$$

for $x \in \Theta_l$, $y \in \theta^x_{l+1}$ and some tolerance tol > 0 to avoid numerical instabilities. With this, we set the coefficients

$$\psi^l_x(y) := \left(\sum_{T \in \mathcal{G}^{y,1}_l} \alpha^l_{x,T,y} \right)^{-1} \sum_{T \in \mathcal{G}^{y,1}_l} \alpha^l_{x,T,y} \, \zeta_{x,T}(y). \tag{23}$$

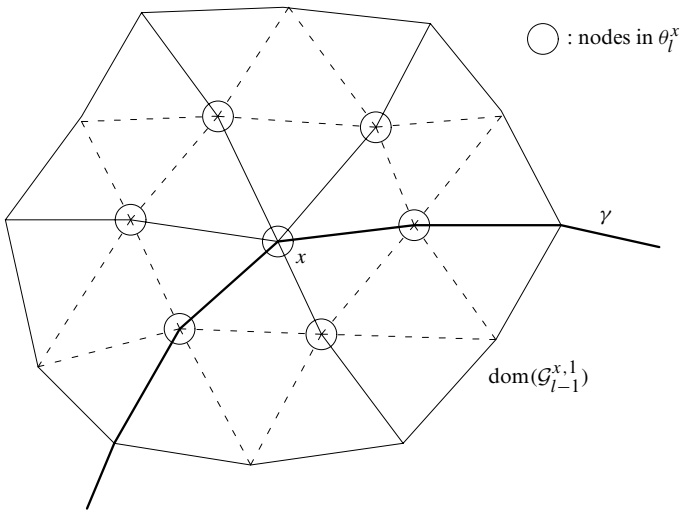

Fig. 4. The set θ^x_l

This determines the coefficients in (15) and, finally, we arrive at (with the coefficients $\psi_x^l(y)$ as in (23))

$$\psi_x^l := \sum_{y \in \theta_{l+1}^x} \psi_x^l(y)\, \psi_y^{l+1}. \tag{24}$$

5.2. Properties of Composite Finite Elements

The construction of the previous sections lead to the definition of the composite finite element spaces for problems with jumping coefficients.

Definition 5.2: *Let Assumption* 5.1 *be satisfied.*

– $l = L$: *On the finest grid* $\mathcal{G}_L$, *the linear finite element Lagrange basis is given by* $\{\psi_x^L\}_{x \in \Theta_L}$ *and the corresponding composite finite element space equals the standard one*

$$\mathcal{S}_L^{\mathrm{CFE}} := \mathcal{S}_L \subset H^1(\Omega).$$

– $l = L-1, L-2, \ldots$
The basis functions $\{\psi_x^l\}_{x \in \Theta_l}$ *are given as in (23), (24) and the space of* composite finite elements $\mathcal{S}_l^{\mathrm{CFE}}$ *is given by*

$$\mathcal{S}_l^{\mathrm{CFE}} := \operatorname{span}\{\psi_x^l : x \in \Theta_l\} \subset H^1(\Omega).$$

Next, we rewrite the steps for computing the finite element basis functions $\{\psi_x^l\}_{x \in \Theta_l}$ for $0 \le l \le L$ in an algorithmic way.

Algorithm 5.3: Let Assumption 5.1 be satisfied and let $\{\psi_x^L\}_{x \in \Theta_L} := \{\varphi_x^L\}_{x \in \Theta_L}$ and $S_L^{\mathrm{CFE}} := \mathcal{S}_L$. Let $k \in \mathbb{N}_0$. For $l = L-1, \ldots, 0$ do

(1) for all $T \in \mathcal{G}_l$ with vertices θ_T compute for all $x \in \theta_T$
  (a) (i) the boundary values $g_{x,T}^l$ by (18),
    (ii) the solutions $u_{x,T}^l \in \mathcal{S}_{l+1}^{\mathrm{CFE}} \cap H_0^1(U_T)$ of (19) and
    (iii) the functions $\xi_{x,T}^l := u_{x,T}^l + g_{x,T}^l$ in U_T,
  (b) the functions $\zeta_{x,T}^l$ by (21) and
  (c) the weights $[\alpha_{x,T}^l]$ by (22),
(2) for all $x \in \Theta_l$, compute ψ_x^l by (24).

Remark 5.4: For the assembling of the linear system, step (2) in Algorithm 5.3 is not required but only the weights $[\alpha_{x,T}^l]$ have to be computed. Such constructions via "mask coefficients" are quite common in wavelet methods.

With (24), it holds $\psi_x^l \in \mathcal{S}_{l+1}^{\mathrm{CFE}}$ for all $x \in \Theta_l$ leading to the nestedness of the spaces:

$$\mathcal{S}_l^{\mathrm{CFE}} \subset \mathcal{S}_{l+1}^{\mathrm{CFE}}.$$

Lemma 5.5: *Let Assumption* 5.1 *be satisfied and let* $0 \le l \le L$.

(1) $\{\psi_x^l\}_{x\in\Theta_l}$ *forms a Lagrange basis.*

(2) *For all* $x \in \Theta_l$, *it holds* $\operatorname{supp}\psi_x^l \subset \operatorname{supp}\varphi_x^l$.

Proof: Both assertions hold for linear finite elements, thus, for the composite finite elements $\{\psi_x^L\}_{x\in\Theta_L}$ on the finest grid $\mathcal{G}_L$. Let $0 \le l < L$ and assume that the assertions hold for $l+1$. Let $x \in \Theta_l$.

1. Inductively, we know that $\{\psi_x^{l+1}\}_{x\in\Theta_{l+1}}$ is a Lagrange basis and conclude $\psi_z^{l+1}(y) = 0$ for all $y \in \Theta_l$ and for all $z \in \Theta_{l+1}\setminus\Theta_l$. Therefore, from

$$\theta_{l+1}^x \subset \{x\} \cup \big(\Theta_{l+1}\setminus\Theta_l\big)$$

and (24), it follows for the coefficient $\psi_x^l(y)$ that

$$\psi_x^l(y) = \sum_{z\in\theta_{l+1}^x} \psi_x^l(z)\,\psi_z^{l+1}(y) = \psi_x^l(x)\,\psi_x^{l+1}(y) = 0$$

for all $x \ne y \in \Theta_l$. Since $\zeta_{x,T}(x) = 1$, we obtain

$$\psi_x^l(x) = \sum_{y\in\theta_{l+1}^x} \left(\sum_{T\in\mathcal{G}_l^{y,1}} \alpha_{x,T,y}^l\right)^{-1} \sum_{T\in\mathcal{G}_l^{y,1}} \alpha_{x,T,y}^l\,\zeta_{x,T}(y)\,\psi_y^{l+1}(x)$$

$$= \left(\sum_{T\in\mathcal{G}_l^{x,1}} \alpha_{x,T,x}^l\right)^{-1} \sum_{T\in\mathcal{G}_l^{x,1}} \alpha_{x,T,x}^l\,\zeta_{x,T}(x) = 1.$$

2. The induction assumption and Assumption 5.1 imply

$$\operatorname{supp}\psi_y^{l+1} \subset \operatorname{supp}\varphi_y^{l+1} \subset \operatorname{supp}\varphi_x^l$$

for all $y \in \theta_{l+1}^x$ and, consequently,

$$\operatorname{supp}\psi_x^l \subset \bigcup_{y\in\theta_{l+1}^x} \operatorname{supp}\psi_y^{l+1} \subset \operatorname{supp}\varphi_x^l.$$

□

Lemma 5.6: *Let Assumption* 5.1 *be satisfied and let the coefficient a be constant, i. e.,* $a(x) = a_0 \in \mathbb{R}_{>0}$ *for all* $x \in \Omega$.

Then, it holds $\psi_x^l = \varphi_x^l$ *for* $0 \le l \le L$ *and* $x \in \Theta_l$.

The proof is elementary and, hence, skipped.

5.3. Laminar Interfaces

For laminar interfaces, e. g., $a(\eta_1, \eta_2) = \tilde{a}(\eta_1)$, tensorized finite elements which consist of linear elements tangential to the internal boundary γ and one-dimensional composite finite elements (as in Sect. 4) in normal direction to γ are well suited for discretizations. To be specific, let $\Omega := (0,1)^2$ and let $x_1 := (0,0)$, $x_2 := (1,0)$, $x_3 := (0,1)$, $x_4 := (1,1)$ denote the nodes of Ω (see Fig. 5). For $a_0 \in \mathbb{R}_{>0}$ and for $x = (\eta_1, \eta_2) \in \mathbb{R}^2$, we consider the discontinuous coefficient

$$a(x) := \begin{cases} 1 & \text{for } \eta_1 \leq \frac{1}{2}, \\ a_0 & \text{for } \eta_1 > \frac{1}{2}. \end{cases}$$

Tensorized (bilinear) finite elements on Ω are given as the span of the four basis functions

$$\begin{aligned} b_1(\eta_1, \eta_2) &= \lambda_1(\eta_1)\,\lambda_2(\eta_2), & b_2(\eta_1, \eta_2) &= (1 - \lambda_1(\eta_1))\,\lambda_2(\eta_2), \\ b_3(\eta_1, \eta_2) &= \lambda_1(\eta_1)\,(1 - \lambda_2(\eta_2)), & b_4(\eta_1, \eta_2) &= (1 - \lambda_1(\eta_1))\,(1 - \lambda_2(\eta_2)), \end{aligned}$$

where

$$\lambda_1(\eta_1) = \begin{cases} -\frac{2a_0}{1+a_0}\,\eta_1 + 1 & \text{for } \eta_1 \in [0, \frac{1}{2}], \\ -\frac{2}{1+a_0}\,\eta_1 + \frac{2}{1+a_0} & \text{for } \eta_1 \in (\frac{1}{2}, 1] \end{cases} \quad \text{and} \quad \lambda_2(\eta_2) = 1 - \lambda_2. \tag{25}$$

Let $u \in H^1(\Omega)$ with $a\,\partial_1 u, \partial_2 u \in H^1(\Omega)$ such that $u(x_1) = u(x_3) = 1$ and $u(x_2) = u(x_4) = 0$. The interpolation of u by these tensorized finite elements is given by

$$\mathcal{I}_{\otimes}^{\mathrm{CFE}} u(x) := \mathcal{I}_{\otimes}^{\mathrm{CFE}} u(\eta_1, \eta_2) := \lambda_1(\eta_1)$$

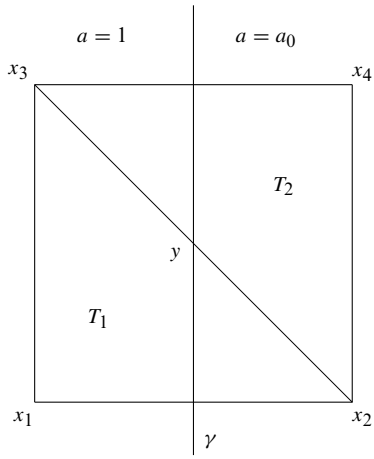

Fig. 5. The domain Ω with the interface γ and the elements T_1 and T_2

which, for $y = (\frac{1}{2}, \frac{1}{2})$, implies

$$\mathcal{I}_{\otimes}^{\mathrm{CFE}} u(y) = \frac{1}{1+a_0} \longrightarrow 0 \quad \text{for } a_0 \to \infty. \tag{26}$$

The construction of tensorized finite elements requires that the interface is aligned with (rectangular) mesh cells which is typically *not* the case for practical applications. However, the weights $\left[\alpha_{x,T}^{l}\right]$ in (22) will be chosen such that, for laminar interfaces, the composite finite element functions approximate these tensorized finite elements.

Let T_1 be the element with vertices x_1, x_2, x_3 and T_2 the one with x_2, x_4, x_3. The functions ζ_{x_3,T_i}, $1 \le i \le 2$, as in (21) are discontinuous across $\overline{x_2 x_3}$. Easy calculations yield

$$\zeta_{x_3,T_1}(x) = \eta_2$$

for $x = (\eta_1, \eta_2) \in \overline{T}_1$, and, for $x = (\eta_1, \eta_2) \in \overline{T}_2$,

$$\zeta_{x_3,T_2}(x) = \lambda_1(\eta_1)$$

with λ_1 as in (25). A basis function $\tilde{\psi}_{x_3}$, which would be computed by an average of these two functions in y with weights $1/2$ from both sides satisfies

$$\tilde{\psi}_{x_3}(y) = \frac{1}{2}\Big(\frac{1}{2} + \frac{1}{1+a_0}\Big) \longrightarrow \frac{1}{4} \quad \text{for } a_0 \to \infty.$$

This differs from the limit in (26). Thus, we require a weighted average that puts more weight on ζ_{x_3,T_2} than on ζ_{x_3,T_1}. Since $[\partial_\nu \zeta_{x_3,T_1}] = [\partial_1 \zeta_{x_3,T_1}] = 0$, it follows:

$$\left[\alpha_{x_3,T_1}\right] = \Big| \int_{\gamma \cap T_1} [a] \left[\partial_\nu \zeta_{x_3,T_1}\right] d\sigma \Big| = 0,$$

and $\left[\alpha_{x_3,T_2}\right] \neq 0$. Let $\mathcal{I}^{\mathrm{CFE}}$ be the interpolation as in (16). Then, the weights $\left[\alpha_{x,T}\right]$ preserve the requested limiting behaviour. The weighted average in (23) gives

$$\mathcal{I}^{\mathrm{CFE}} u(y) = \psi_{x_3}(y) = \left[\alpha_{x_3,T_2}\right]^{-1} \left[\alpha_{x_3,T_2}\right] \frac{1}{1+a_0} = \mathcal{I}_{\otimes}^{\mathrm{CFE}} u(y).$$

5.4. Efficient Realization

Analogously to (4), we define the prolongation via the composite finite elements. The restriction is given by the transposed of the prolongation. Although the composite finite elements have a complicated structure on the coarser grids, the prolongation is a local operation and can be realized by local, purely algebraic transformations. Thus, one multigrid iteration has a complexity of order $O(\#\Theta_L)$.

We compute these matrices in an initialization step before the multigrid algorithm is performed. The complexity of this initialization step is of order $O(\#\Theta_L)$ as well.

For all $0 \le l \le L$, we introduce the set of inner grid points

$$\Theta_l^0 := \Theta_l \cap \Omega$$

which are associated to the degrees of freedom. Then, $\{\psi_x^l\}_{x\in\Theta_l^0}$ is a basis of $\mathcal{S}_l^{\mathrm{CFE}} \cap H_0^1(\Omega)$. We identify this space with the space $\mathbb{R}^{\Theta_l^0}$ via this basis.

In analogy to (4) respectively (5), we define the prolongation P_l^{l+1} by

$$\begin{aligned} P_l^{l+1} &: \mathbb{R}^{\Theta_l^0} \to \mathbb{R}^{\Theta_{l+1}^0}; \\ \left(P_l^{l+1}U\right)_x &:= \textstyle\sum_{y\in\Theta_l^0} \psi_y^l(x)\, U_y \quad \text{for all } x \in \Theta_{l+1}^0 \end{aligned} \tag{27}$$

and the restriction R_{l+1}^l by

$$\begin{aligned} R_{l+1}^l &:= \left(P_l^{l+1}\right)^T : \mathbb{R}^{\Theta_{l+1}^0} \to \mathbb{R}^{\Theta_l^0}; \\ \left(R_{l+1}^l U\right)_x &:= \sum_{y\in\Theta_{l+1}^0} \psi_x^l(y)\, U_y \qquad \text{for all} \quad x \in \Theta_l^0. \end{aligned} \tag{28}$$

Let b be the bilinear form as in (1). Then, the system matrices A_l, $0 \le l \le L$, are given by

$$(A_l)_{x,y} := b(\psi_y^l, \psi_x^l) \tag{29}$$

for all $x, y \in \Theta_l^0$. Equivalently, the matrices on the coarser grids $\mathcal{G}_l$, $0 \le l < L$, can be represented by the Galerkin products

$$A_l := R_{l+1}^l\, A_{l+1}\, P_l^{l+1} \tag{30}$$

which is more appropriate for the actual computation of these matrices than (29).

The matrix A_{l+1} can conveniently be used for the computation of the finite elements $\{\psi_x^l\}_{x\in\Theta_l^0}$, i. e., the computation of the prolongation P_l^{l+1}. Therefore, we link the computation of the prolongation with the products from (30).

The following integrals are used for the computation of the weights $[\alpha_{x,T}^l]$. For $x \in \Theta_l$ and the edges e of the grids $\mathcal{G}_l$, set

$$I_{x,e}^l := \int_e [a]\left[\partial_\nu \psi_x^l\right] d\sigma \tag{31}$$

and, for $T \in \mathcal{G}_l$, set

$$I_{x,T}^l := \int_{\gamma\cap T} [a]\left[\partial_\nu \psi_x^l\right] d\sigma. \tag{32}$$

Let Assumption 5.1 be satisfied. Then, the composite finite elements $\{\psi_x^L\}_{x\in\Theta_L^0}$ on the finest grid $\mathcal{G}_L$ are linear finite elements. Thus, the system matrix A_L as well as the integrals in (31) and (32) can easily be computed.

Let $0 \le l < L$ and assume that the system matrix A_{l+1} and the integrals $I_{x,e}^{l+1}$ and $I_{x,T}^{l+1}$ for $x \in \Theta_{l+1}$, $T \in \mathcal{G}_{l+1}$ and the edges e of the grid $\mathcal{G}_{l+1}$ are given. Furthermore, we require the values $(A_{l+1})_{x,y} = b(\psi_y^{l+1}, \psi_x^{l+1})$ for all $x, y \in \Theta_{l+1}$ because these additional values in the nodes $\Theta_{l+1} \setminus \Theta_{l+1}^0$ on the boundary $\partial\Omega$ are needed for the computation of the functions $\xi_{x,T}^l$ in (20).

Let $T \in \mathcal{G}_l$, $x \in \Theta_l \cap \overline{T}$ and let $\mathcal{E}_T$ be the set of (open) edges of $\mathcal{G}_{l+1}$ that lie in T. Then, the initialization consists of the following steps:

(1) Let $g_{x,T}^l$ be as in (18). Then,

$$\left\{\xi_{x,T}^l(y)\right\}_{y \in \Theta_{l+1} \cap U_T} \tag{33}$$

is the solution of a system of linear equations with coefficients $A_{l+1,zy} = b(\psi_y^{l+1}, \psi_z^{l+1})$ with $z \in \Theta_{l+1} \cap U_T$. Note that, for all $y \in \Theta_{l+1} \cap \partial U_T$, the values $\xi_{x,T}^l(y)$ are prescribed by $g_{x,T}^l(y)$.

(2) The weights $\left[\alpha_{x,T}^l\right]$ are given by

$$\left[\alpha_{x,T}^l\right] = \left| \sum_{y \in \Theta_{l+1} \cap \overline{T}} \zeta_{x,T}^l(y) \left(\sum_{S \in \operatorname{sons}(T)} I_{y,S}^{l+1} + \sum_{e \in \mathcal{E}_T} I_{y,e}^{l+1} \right) \right|. \tag{34}$$

(3) Let e be an edge of the grid $\mathcal{G}_l$ and let $\mathcal{E}_e$ be the set of edges of $\mathcal{G}_{l+1}$ such that

$$\bigcup_{e' \in \mathcal{E}_e} \overline{e'} = \overline{e}.$$

Then, it holds

$$I_{x,e}^l = \sum_{z \in \Theta_{l+1} \cap \operatorname{dom}(\mathcal{G}_l^{x,1})} \psi_x^l(z) \sum_{e_{l+1} \in \mathcal{E}_e} I_{z,e_{l+1}}^{l+1} \tag{35}$$

as well as

$$I_{x,T}^l = \sum_{z \in \Theta_{l+1} \cap \operatorname{dom}(\mathcal{G}_l^{x,1})} \psi_x^l(z) \left(\sum_{S \in \operatorname{sons}(T)} I_{z,S}^{l+1} + \sum_{e \in \mathcal{E}_T} I_{z,e}^{l+1} \right). \tag{36}$$

The different steps of this initialization are summarized below.

Algorithm 5.7: Let Assumption 5.1 be satisfied.

(1) Compute A_L as in (29).
(2) For $x \in \Theta_L$ and the edges e of the grid $\mathcal{G}_L$, compute the integrals $I_{x,e}^L$ as in (31) and set $I_{x,T}^L = 0$ for all $T \in \mathcal{G}_L$.

(3) For $l = L-1, \dots, 0$, compute
   (a) for $x \in \Theta_l$ and $y \in \Theta_{l+1}$ the values $\psi_x^l(y)$ (cf. (24)) (with the auxiliary functions $\xi_{x,T}^l$ from (20) and $\zeta_{x,T}^l$ from (21) and with the weights $\left[\alpha_{x,T}^l\right]$ from (22)),
   (b) the prolongation P_l^{l+1} and the restriction R_{l+1}^l (cf. (27)), respectively (28) including their local versions,
   (c) the system matrix $A_l = R_{l+1}^l\, A_{l+1}\, P_l^{l+1}$, and
   (d) the integrals $I_{x,e}^l$ and $I_{x,T}^l$ as in (35), respectively (36) for $x \in \Theta_l$, the edges e of the grid $\mathcal{G}_l$ and $T \in \mathcal{G}_l$.
   (e) restrict all matrices to $\Theta_l^0 \subset \Theta_l$.

Note that all steps in Algorithm 5.7(3) can be realized by local operators and all arising matrices are sparse.

In order to estimate the computational work of this initialization, we have to restrict the number of successor and neighbours of the elements.

Assumption 5.8: *There exists a number $\delta \in \mathbb{N}$ such that, for all $0 \le l < L$ and all $T \in \mathcal{G}_l$, it holds*

$$\#\,\mathrm{sons}(T) < \delta.$$

For all $0 \le l \le L$ and all $x \in \Theta_l$, it holds

$$\#\mathcal{G}_l^{x,1} \le \delta. \tag{37}$$

There exists a constant $\eta \in (0,1)$ such that, for all $0 \le l < L$,

$$\#\Theta_l \le \eta\ \#\Theta_{l+1}.$$

This assumption guarantees that the number of elements in the zones U_T is bounded independently of the refinement level l of $\mathcal{G}_l$. Of course, the complexity depends strongly on the number of "layers" k which are employed for determining the size of the security zones. More precisely, it holds $\#\mathcal{G}_l^{T,k} = O(\delta^k)$ by Assumption 5.8 with δ from (37). This implies that the dimension of the linear systems in (33) is also bounded independently of l. In general, it is not very large as we choose $k \in \{1, 2, 3\}$. Therefore, these systems can be solved by LU-factorization or, in the case of our symmetric model problem, by the Cholesky factorization.

The product $R_{l+1}^l\, A_{l+1}\, P_l^{l+1}$ can be computed efficiently by the multiplication with unit vectors. In an implementation of this algorithm, we require therefore "local" versions of the matrix-vector-multiplications for the three matrices.

Lemma 5.9: *Let Assumptions* 5.1 *and* 5.8 *be satisfied and let $k \in \mathbb{N}_0$ be the number of "layers" in the security zones* (*cf.* (17)).

Then, the complexity of the initialization in Algorithm 5.7 is of order $O\left(\delta^{3k+3}\frac{\eta}{1-\eta}\#\Theta_L\right)$.

Proof: The following numbering corresponds to the numbering of Algorithm 5.7. 1. and 2. The computation of A_L and the integrals $I^L_{x,e}$ has a complexity of order $O(\delta\,\#\Theta_L)$. 3. Let $0 \le l < L$. a) There are three linear systems to solve for each element $T \in \mathcal{G}_l$ to obtain the values $\xi^l_{x,T}(y)$ in (33). The dimension of these systems is of order $O(\delta^{k+1})$. Using LU- or Cholesky factorization, this has a complexity of order $O\big(\delta^{3k+3}\big)$. Summarizing, the complexity is of order $O\big(\delta^{3k+3}\,\#\Theta_l\big)$. The complexity to compute the sums in (34) is of order $O(\delta^2\,\#\Theta_l)$. Finally, the coefficients $\psi^l_x(y)$ are computed by (24) which sums up to a complexity of order $O(\delta^{k+1}\,\#\Theta_l)$. *c)* We compute the columns of A_l by evaluating the product $R^l_{l+1}\,A_{l+1}\,P^{l+1}_l$ for all unit vectors Ψ^l_x. By (27), there are $O(\delta^2)$ components of the vector $P^{l+1}_l\Psi^l_x$ that do not vanish. In each row of A_{l+1}, there are at most $\delta+1$ components not vanishing and in each row of R^l_{l+1}, there are three by (28) and by Lemma 5.5 (2). Thus, the complexity to compute A_l is of order $O(\delta^2\,\#\Theta_l)$. *d)* The computation of the integrals $I^l_{x,e}$ and $I^l_{x,T}$ in (35) respectively (36) has a complexity of order $O(\delta^2\,\#\Theta_l)$. For fixed l, the complexity of Step 3 is of order $O\big(\delta^{3k+3}\,\#\Theta_l\big)$. Since $\#\Theta_l \le \eta\ \#\Theta_{l+1}$, it follows $\#\Theta_l \le \eta^{L-l}\,\#\Theta_L$. This implies

$$\sum_{l=0}^{L-1} \#\Theta_l \le \#\Theta_L \sum_{l=0}^{L-1} \eta^{L-l} \le \#\Theta_L \sum_{l=1}^{\infty} \eta^l = \#\Theta_L\,\frac{\eta}{1-\eta}.$$

Typically, we choose $k \in \{1, 2, 3\}$. If $\#\mathcal{G}_0$ is of order $O(1)$ and congruent refinement is used recursively for the refinement of the grids then δ is of order $O(1)$ and η is about $1/4$. Hence, the complexity of the initialization is of order $O(\#\Theta_L)$.

6. Numerical Results

We have implemented the CFE–MG from Sect. 5 for Problem 2.1 in two dimensions. This implementation allows us to study the dependence of the multigrid method on the coefficient a. We consider an example with periodic coefficients which allows to perform various parameter tests. However, the periodic structure is not at all required for the composite finite elements and is just for the purpose of systematic parameter studies.

In this section, we consider the domain $\Omega := (0,1)^2$ and the right-hand side $f = 1$. We employ the following hierarchy of grids on this domain. The coarsest grid $\mathcal{G}_0$ consists of the two triangles with vertices $(0,0)$, $(1,0)$, $(0,1)$, respectively $(1,0)$, $(1,1)$, $(0,1)$ (see Fig. 6). For $l \in \mathbb{N}$, the grids $\mathcal{G}_l$ are given by recursive congruent refinement of the grid $\mathcal{G}_0$. Then, it holds $h_l = 2^{1/2-l}$.

We set

$$\omega := \operatorname{int}\big(\operatorname{conv}\big\{(\tfrac14,\tfrac34),(\tfrac14,\tfrac12),(\tfrac12,\tfrac14),(\tfrac34,\tfrac14),(\tfrac34,\tfrac12),(\tfrac12,\tfrac34)\big\}\big)$$

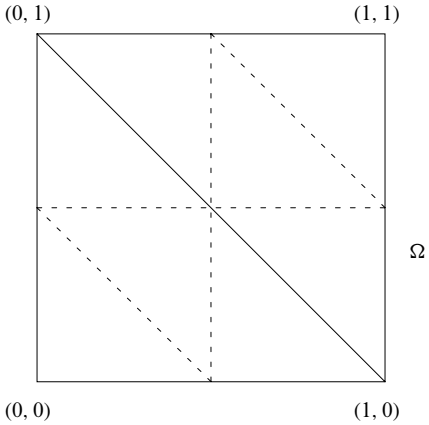

Fig. 6. The grids $\mathcal{G}_0$ and $\mathcal{G}_1$ on the domain $\Omega = (0, 1)^2$

(see Fig. 7). For $a_0 > 0$ and $x \in [0, 1]^2$, set

$$a(x) := \begin{cases} a_0 & \text{for } x \in \omega, \\ 1 & \text{otherwise} \end{cases}$$

and extend $a(\cdot)$ periodically with period 1 onto $\mathbb{R}^2$. For $\varepsilon \in (0, 1]$ and for $x \in \mathbb{R}^2$, set

$$a^\varepsilon(x) := a(x/\varepsilon).$$

We always use the security zones $U_T = \mathrm{dom}(\mathcal{G}_l^{T,2})$, i. e., two "layers" of elements. Let $u_l^\varepsilon \in \mathcal{S}_l^{\mathrm{CFE}} \cap H_0^1(\Omega)$ be the solution of the discrete Problem 2.2 corresponding

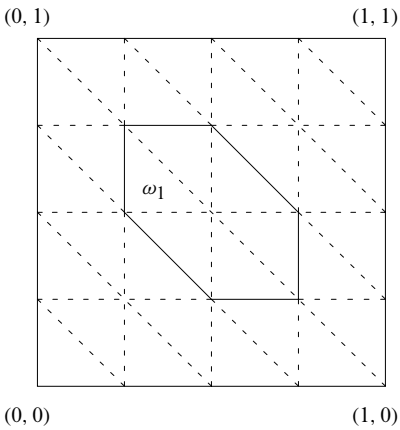

Fig. 7. The unit cell with the domain ω

to the coefficient a^ε. For $i \in \mathbb{N}_0$, let $\varepsilon_i := 2^{-i}$. Then, the coefficient a^{ε_i} is resolved by the grid $\mathcal{G}_l$ for $l \geq i + 2$.

In Fig. 8, two basis functions at the node $x = (\frac{1}{2}, \frac{1}{2})$ are displayed on different grids. We have chosen $a_0 = 50$ and $\varepsilon = \frac{1}{8}$. The left function is ψ_x^3 on $\mathcal{G}_6$ and the right one is the function ψ_x^2. Figure 9 shows the solution u_6^ε of the associated problems on the grid $\mathcal{G}_6$. Again, we have chosen $\varepsilon = \frac{1}{8}$. The left solution corresponds to $a_0 = \frac{1}{50}$ and the right one to $a_0 = 50$.

In the following, we study the dependence of the multigrid convergence rate on the coefficient a. For the iteration, we use the initial function $u_l^{\varepsilon_i,0} = 0$. We denote the

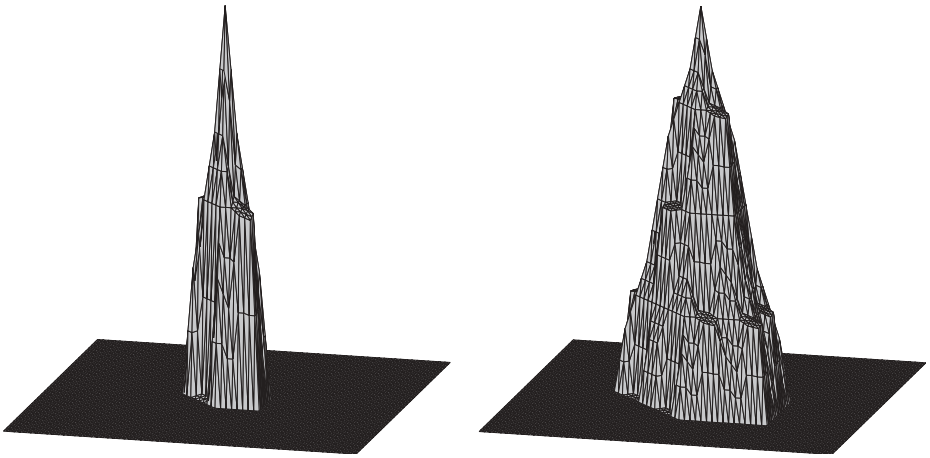

Fig. 8. The basis functions ψ_x^3 and ψ_x^2 on the grid $\mathcal{G}_6$ with $a_0 = 50$ and $\varepsilon = \frac{1}{8}$

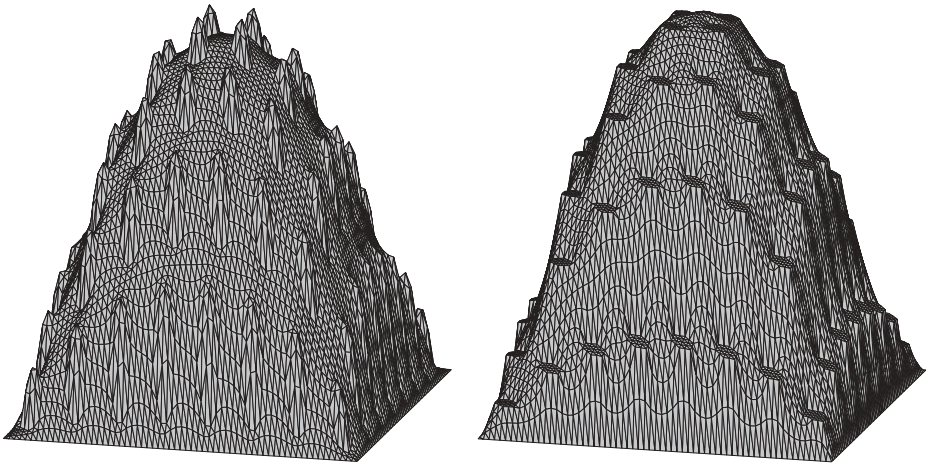

Fig. 9. The solutions u_6^ε on the grid $\mathcal{G}_6$ with $a_0 = \frac{1}{50}$ respectively $a_0 = 50$, with $\varepsilon = \frac{1}{8}$ each

resulting function after n iteration steps by $u_l^{\varepsilon_i,n}$. Then, the convergence rate r_{i,l,a_0} is given by the mean value of the quotients

$$\frac{\|A_l u_l^{\varepsilon_i,n} - f\|_{L^2(\Omega)}}{\|A_l u_l^{\varepsilon_i,n-1} - f\|_{L^2(\Omega)}}. \tag{38}$$

All computations are done with two pre- and two post-smoothing steps with the symmetric Gauß-Seidel iteration and with the V-cycle. The iteration is stopped if the L^2-norm of the residuum $\|A_l u_{p,l}^{\varepsilon_i,n} - f\|_{L^2(\Omega)}$ is smaller than 10^{-10}.

In Tables 1–4, the convergence rates r_{i,l,a_0} of the multigrid method are given with $l = i + q$, $2 \le q \le 5$, for different a_0 each. In order to study the dependence on ε, the tables are ordered by ε_i respectively $1/\varepsilon_i = 2^i$. The grid level l can be determined by

$$l = i + q = q - \log_2(\varepsilon_i).$$

Table 1. Convergence rates for grid levels $l = 2 - \log_2(\varepsilon_i) = 3, \ldots, 9$

$r_{1,i,i+2,a_0}$		$1/\varepsilon_i$						
		2	4	8	16	32	64	128
a_0	1	0.07	0.09	0.09	0.10	0.10	0.10	0.10
	10^{-3}	0.08	0.12	0.14	0.15	0.16	0.16	0.16
	10^{-6}	0.08	0.12	0.14	0.15	0.16	0.16	0.16
	10^{3}	0.18	0.17	0.15	0.13	0.13	0.13	0.13
	10^{6}	0.19	0.18	0.16	0.13	0.13	0.13	0.13

Table 2. Convergence rates for grid levels $l = 3 - \log_2(\varepsilon_i) = 4, \ldots, 10$

$r_{1,i,i+3,a_0}$		$1/\varepsilon_i$						
		2	4	8	16	32	64	128
a_0	1	0.09	0.09	0.09	0.10	0.10	0.10	0.10
	10^{-3}	0.13	0.16	0.19	0.20	0.21	0.21	0.21
	10^{-6}	0.13	0.16	0.19	0.20	0.21	0.21	0.21
	10^{3}	0.26	0.24	0.21	0.19	0.18	0.17	0.17
	10^{6}	0.26	0.25	0.23	0.19	0.18	0.17	0.17

Table 3. Convergence rates for grid levels $l = 4 - \log_2(\varepsilon_i) = 5, \ldots, 11$

$r_{1,i,i+4,a_0}$		$1/\varepsilon_i$						
		2	4	8	16	32	64	128
a_0	1	0.10	0.10	0.10	0.10	0.10	0.10	0.10
	10^{-3}	0.16	0.18	0.21	0.22	0.23	0.23	0.23
	10^{-6}	0.16	0.18	0.21	0.22	0.23	0.23	0.23
	10^{3}	0.28	0.26	0.23	0.21	0.19	0.19	0.20
	10^{6}	0.29	0.28	0.26	0.22	0.20	0.20	0.20

Table 4. Convergence rates for grid levels $l = 5 - \log_2(\varepsilon_i) = 6, \ldots, 12$

$r_{1,i,i+5,a_0}$		$1/\varepsilon_i$						
		2	4	8	16	32	64	128
a_0	1	0.10	0.10	0.10	0.10	0.10	0.10	0.10
	10^{-3}	0.17	0.19	0.22	0.23	0.23	0.24	0.24
	10^{-6}	0.17	0.19	0.22	0.23	0.23	0.24	0.24
	10^{3}	0.29	0.26	0.24	0.21	0.21	0.21	0.21
	10^{6}	0.31	0.29	0.25	0.22	0.22	0.22	0.22

Table 5. Run times (in seconds) of the program on different grids $\mathcal{G}_l$

Level l	DoF_l	$\frac{\mathrm{DoF}_l}{\mathrm{DoF}_{l-1}}$	T_l^{Init}/s	$\frac{T_l^{Init}}{T_{l-1}^{Init}}$	T_l^{MGM}/s	$\frac{T_l^{MGM}}{T_{l-1}^{MGM}}$	T_l^{All}/s	$\frac{T_l^{All}}{T_{l-1}^{All}}$
4	225	–	1.47	–	0.01	–	1.49	–
5	961	4.27	2.74	1.86	0.04	4.00	2.80	1.88
6	3969	4.13	9.87	3.60	0.16	4.00	10.19	3.64
7	16129	4.06	42.98	4.35	0.92	5.75	44.63	4.38
8	65025	4.03	168.85	3.93	8.67	9.42	180.94	4.05
9	261121	4.02	679.70	4.03	46.03	5.31	740.22	4.09
10	1046529	4.01	2756.36	4.06	219.37	4.77	3033.97	4.10
11	4190209	4.00	11071.75	4.02	866.82	3.95	12172.24	4.01

In Table 1, the values, for instance, correspond to the grid levels $l = 3, \ldots, 9$.

The computations show that the convergence rates are larger than for the Poisson problem ($a_0 = 1$), but, more importantly, they are still small and show clearly that they are bounded by approximately 0.3 for all test cases independently of the various parameters, in particular independent of ε.

The computations are done on a SunFire 6800 with 16 CPUs (UltraSparc III with 900 MHz) and 16 GByte shared memory. The given run times are always "user" times, i. e., the total run time of all CPUs. The main part of the initialization step consists of the solution of local problems leading to small linear systems. In order to solve them, we use the Cholesky factorization of Lapack. The systems are independent of each other and can be solved in parallel.

The complexity of both the initialization step (cf. Subsect. 5.4) as well as the multigrid method is linear in the degrees of freedom on the finest grid. The run times of our program are given in Table 5 ("user" times in seconds) on different grids $\mathcal{G}_l$. There, T_l^{Init} refers to the run time of the initialization step, T_l^{MGM} corresponds to the run time of ten multigrid iterations and T_l^{All} is the total run time of the program. The computations are done with the parameters $l = i + 2$ and $a_0 = 1$ which have no influence on the run times per iteration step.

The quotients of the run times match the quotients of the degrees of freedom very well. This shows that the complexity of our implementation confirms the theoretically predicted linear complexity.

The quite large quotients for the multigrid method for middle-sized grids might issue from data outgrowing the cache. The quotients for the larger grids are again consistent with the linear complexity.

Acknowledgement

The second author was partially supported by the European Research Training Network "Homogenization and Multiple Scales" (HMS2000).

References

[1] Babuška, I.: The finite element method for elliptic equations with discontinuous coefficients. Computing *5*, 207–213 (1970).
[2] Babuška, I., Andersson, B., Smith, P. J., Levin, K.: Damage analysis of fiber composites. I: Statistical analysis of fiber scale. Comput. Meth. Appl. Mech. Engng. *172*, 27–77 (1999).
[3] Babuška, I., Caloz, G., Osborn. J. E.: Special finite element methods for a class of second-order elliptic problems with rough coefficients. SIAM J. Numer. Anal. *31(4)*, 945–981 (1994).
[4] Babuška, I., Osborn. J. E.: Can a finite element method perform arbitrarily badly? Math. Comp. *69(230)*, 443–462 (2000).
[5] Ciarlet, P. G.: The finite element method for elliptic problems. Amsterdam: North-Holland 1987.
[6] Cioranescu, D., Saint Jean Paulin, J.: Homogenization of reticulated structures. New York: Springer 1999.
[7] Frauböse, N., Sauter, S.: Composite finite elements and multigrid. Part I: Convergence theory in 1-d. Proc. 17th GAMM-Seminar Leipzig on Construction of Grid Generation Algorithms, MPI Leipzig, 2001.
[8] Hackbusch, W.: Multi-grid methods and applications. Berlin Heidelberg: Springer 1985.
[9] Hackbusch, W., Sauter, S. A.: Adaptive composite finite elements for the solution of PDEs containing nonuniformly distributed micro-scales. Mater. Model. *8*, 31–43 (1996).
[10] Hackbusch, W., Sauter, S. A.: Composite finite elements for the approximation of PDEs on domains with complicated micro-structures. Numer. Math. *75(4)*, 447–472 (1997).
[11] Hackbusch, W., Sauter, S. A.: Composite finite elements for problems containing small geometric details. Part II: Implementation and numerical results. Comput. Visual Sci. *1*, 15–25 (1997).
[12] Hackbusch, W., Sauter, S. A.: New finite element approach for problems containing small geometric details. Arch. Math. *34(1)*, 105–117 (1998).
[13] Hou, T., Wu, X.-H.: A multiscale finite element method for elliptic problems in composite materials and porous media. J. Comput. Phys. *134(1)*, 169–189 (1997).
[14] Jikov, V. V., Kozlov, S. M., Oleinik, O. A.: Homogenization of differential operators and integral functionals. Berlin Heidelberg: Springer 1994.
[15] Matache, A. M., Babuška, I., Schwab, C.: Generalized *p*-FEM in homogenization. Numer. Math. *86(2)*, 319–375 (2000).
[16] Neuss, N., Jäger, W., Wittum, G.: Homogenization and multigrid. Computing *66(1)*, 1–26 (2001).
[17] Melenk, J. M., Babuška, I.: The partition of unity finite element method: basic theory and applications. Comput. Meth. Appl. Mech. Engng. *139(1–4)*, 289–314 (1996).
[18] Oleinik, O., Shamaev, A., Yosifian, G.: Mathematical problems in elasticity and homogenization. Amsterdam: North-Holland 1992.
[19] Sauter, S. A.: Vergröberung von Finite-Elemente-Räumen. Habilitationsschrift, Christian-Albrechts-Universität zu Kiel, 1997.
[20] Sauter, S. A., Warnke, R.: Extension operators and approximation on domains containing small geometric details. East-West J. Numer. Math. *7(1)*, 61–77 (1999).
[21] Warnke, R.: Schnelle Löser für elliptische Randwertprobleme mit springenden Koeffizienten. Diss. thesis, Universität Zürich, 2003.

S. A. Sauter
Institut für Mathematik
Universität Zürich
Winterthurerstr. 190
8057 Zürich
Switzerland
e-mail: stas@math.unizh.ch

R. Warnke
msg systems ag
Robert-Bürkle-Straße 1
85737 Ismaning
Germany
e-mail: rwarnke@amath.unizh.ch